Coordination Chemistry Reviews 368 (2018) 80–92

Contents lists available at ScienceDirect

Coordination Chemistry Reviews

journal homepage: www.elsevier.com/locate/ccr

Review

Metal-organic frameworks for highly efficient heterogeneous Fenton-like catalysis

Min Cheng [a,b,1], Cui Lai [a,b,1], Yang Liu [a,b,1], Guangming Zeng [a,b,*], Danlian Huang [a,b,*], Chen Zhang [a,b], Lei Qin [a,b], Liang Hu [a,b], Chengyun Zhou [a,b], Weiping Xiong [a,b]

[a] College of Environmental Science and Engineering, Hunan University, Changsha, Hunan 410082, China
[b] Key Laboratory of Environmental Biology and Pollution Control (Hunan University), Ministry of Education, Changsha, Hunan 410082, China

ARTICLE INFO

Article history:
Received 12 December 2017
Accepted 13 April 2018

Keywords:
Metal-organic frameworks
Fenton-like
Wastewater
Organic pollutant
Catalysis

ABSTRACT

The heterogeneous Fenton-like reaction is an advanced oxidation process which has gained wide spread acceptance for high removal efficiency of recalcitrant organic contaminants. Recently, the use of metal-organic frameworks (MOFs) or MOF composites as catalysts for Fenton-like catalysis has received increasing attention due to their permanent porosity and tunable open metal centers. In this article, we present an overview of the development and progress in the synthesis of different types of MOF-based catalysts and their applications for Fenton-like oxidation of organic pollutants. Special attention has been paid to the catalytic mechanism, namely the production of reactive species on the surface of the catalysts. Representative studies in this area were comprehensively reviewed. Overall, it is concluded that several classes of MOF materials with fixed metal centers are able to catalytically degrade organic pollutants over a wide pH range. Meanwhile, research in this field is still at an early stage, many improvements are required before the technology can be efficiently scaled-up and put into practice.

Contents

1. Introduction

Water pollution is one of the most important environmental problems in the world. Large amounts of synthetic organic contaminants, such as pharmaceuticals and personal care products (PPCPs), pesticides and dyes are released daily into different types of wastewaters and ultimately enter into natural water bodies [1–6]. It is well known the vast majority of these compounds are persistent organic pollutants (POPs), owing to their high stability to sunlight irradiation and resistance to microbial attack [7–10]. Many POPs are able to cause damage to living organisms, including human beings [11–14]. Thus, it is imperative to develop an effective method for eliminating these compounds from the environment. Advanced oxidation processes (AOPs) have been demonstrated to achieve good results for the elimination of organic pollutants from wastewater with very short treatment times [15–17]. AOPs are environmentally friendly chemical, electrochem-

* Corresponding authors at: College of Environmental Science and Engineering, Hunan University, Changsha, Hunan 410082, China.
E-mail addresses: zgming@hnu.edu.cn (G. Zeng), huangdanlian@hnu.edu.cn (D. Huang).
[1] These authors contributed equally to this article.

https://doi.org/10.1016/j.ccr.2018.04.012
0010-8545/

ical or photochemical methods sharing the common feature of the in-situ production of the highly active hydroxyl radical (**.**OH) as their main oxidizing agent [7].

The Fenton process has attracted considerable attention in the field of environmental remediation [18–21]. In the classical Fenton reaction (Eq. (1)), the ferrous ions (Fe^{2+}) catalyze the decomposition of hydrogen peroxide (H_2O_2), resulting in the generation of **.**OH radicals [22]. The formed ferric ions (Fe^{3+}) can be reduced through Eq. (2), which is known as a Fenton-like reaction [23,24]. The **.**OH radicals generated from the Fenton reaction are the second most reactive chemical species, they can initiate the decomposition of organic pollutants by hydrogen abstraction (Eq. (3)) or hydroxyl addition (Eq. (4)) [19].

$$Fe^{2+} + H_2O_2 \rightarrow Fe^{3+} + HO^- + \mathbf{.}OH \quad (1)$$

$$Fe^{3+} + H_2O_2 \leftrightarrows Fe^{2+} + H^+ + HO_2\mathbf{.} \quad (2)$$

$$RH + \mathbf{.}OH \rightarrow H_2O + R\mathbf{.} \rightarrow \text{further oxidations} \quad (3)$$

$$R + \mathbf{.}OH \rightarrow \mathbf{.}ROH \rightarrow \text{further oxidations} \quad (4)$$

Following the pioneering practical use of the Fenton reaction for the degradation of organic compounds in the 1930s [22], the Fenton reaction and its derivative technologies, such as electro-Fenton [25–28] and photo-Fenton [29–31], have been extensively studied for the decomposition of numerous organic pollutants. Since mass transfer limitations are negligible in homogeneous Fenton oxidation systems, the reaction can work very effectively during the degradation process [32]. However, the traditional Fenton process suffers from some drawbacks, such as the need for strict pH regulation (pH 2.8–3.5) [33], sludge generation [34] and the loss of the catalyst in the effluent [35]. In order to overcome these drawbacks, heterogeneous Fenton-like processes using solid catalysts have been developed. In heterogeneous Fenton-like catalysis, iron (or other transition metals) is stabilized on/in the catalyst's structure and thus can reduce hydroxide precipitation over a wider pH range [36–39]. Several reviews have summarized a wide range of materials that have been used as catalysts or metal supports in heterogeneous Fenton-like processes [40–44]. These reviews highlight that the development of new types of heterogeneous catalysts with low cost, high activity, good stability and environmental benignancy is important, yet challenging.

Metal-organic frameworks (MOFs), also called porous coordination networks (PCNs) [45,46], or porous coordination polymers (PCPs) [47,48], are crystalline inorganic–organic hybrids assembled from organic ligands and metal ions (or clusters) [49]. MOFs not only combine the respective beneficial characteristics of inorganic and organic components, but also often exhibit unique properties that exceed the expectations for a simple mixture of the components [50,51]. Besides, MOF materials can be designed with dimensions, textural characteristics and specific structures to meet the need of a specific application [52]. Early efforts in this research area were mainly focused on the synthesis of new MOF materials [53–55]; however, in recent years the search for potential applications has been a topic of much interest. [52,56–58]. Since their discovery in the late 1990s [59], MOFs have influenced many fields, such as separation [60], energy storage [61], sensing [61] and catalysis [62].

The occurrence of MOFs opens up new opportunities for the development of catalysts with excellent characteristic features, such as chemical tenability, well-defined structure, large pore volume and high specific area [52,63]. To date, various MOF-derived catalysts have been reported. Moreover, an increasing number of review articles on this topic have appeared in recent years [64–72]. For example, Wen et al. [64] systematically reviewed the recent progress in the design and architectures of MOF-involved H_2 production systems. In a more recent one, Zhu et al. [71] summarized the synthesis, structures and photocatalytic applications of titanium-based MOFs.

The past few years have witnessed rapid progress in MOF-derived Fenton-like catalysts. To date, various MOF-derived Fenton-like catalysts, including single metal (e.g. Fe, Co, Cu) and multiple metal (e.g. Fe/Co, Fe/Cu) containing MOFs, have been reported. The growing number of publications on this topic suggests that MOF-based Fenton-like catalysis will play a significant role in the elimination of organic pollutants. Several review papers [73–76] have mentioned the performance of MOF-based Fenton-like catalysis. To the best of our knowledge, however, MOFs for Fenton-like catalysis and the related mechanism have never been reviewed to date. Therefore, a review summarizing MOFs-based Fenton-like reactions is highly expected.

This review aims at giving an account of the fundamental aspects of MOF-based Fenton-like catalysis. Sections 2–4 discuss the synthesis of different types of MOF-derived catalysts and their application for the Fenton-like oxidation of organic pollutants. Special attention has been paid to the catalytic mechanism and the effects of structure on the catalytic activity of MOF-based catalysts. Section 5 introduces the effects of the initial pH on the performance of MOF-based Fenton-like catalysis. Afterward, the stability and reusability of MOF-based Fenton-like catalysts are presented in Section 6. Section 7 provides a conclusion of the review and finally, the outlooks of these emerging technologies are given for plausible research directions.

2. Fe-based MOFs for heterogeneous Fenton-like catalysis

Among the various types of reported MOFs, Fe-based MOFs showed great potential as heterogeneous Fenton-like catalysts. This is because Fe is non-toxic, abundant in earth crust minerals and Fe-based MOFs show an intensive absorption in the visible light region due to the existence of iron-oxo (Fe-O) clusters [77,78]. To date, a vast number of Fe-based MOFs have been developed, employing multiple types of organic ligands. Bipyridine is one of the most widely used ligands because of the oxidative resistance of the pyridine ring to **.**OH radicals and its strong binding affinity with the Fe^{2+} ion [79,80]. Also, recent progress has shown that the introduction of a carboxyl group to the 2,2′-bipyridine ligand can further stabilize the obtained complex, which is because the carboxyl group could bind with the Fe^{3+} ion formed in the catalytic cycle, avoiding its hydrolyzation. As reported by Li et al. [81], a Fe(II) MOF material (Fe-bpydc) was successfully synthesized with 2,2′-bipyridine-5,5′-dicarboxylate as the ligand and exhibited high catalytic activity for H_2O_2 at near neutral pH conditions. The total turnover number (TON) of a three cycles degradation is 23, revealing its activity and stability are superior to most of the reported MOF catalysts [81]. The ligands can also affect the catalytic performance of Fe-based MOF catalysts by affecting the spatial structure of the MOFs [77,82]. For instance, MIL-100(Fe) (Figs. 1 and 3D, with 1,3,5-benzenetricarboxylic acid as the ligand) showed a much more intensive absorption in the visible light region and higher catalytic ability as compared with MIL-68(Fe) (Figs. 1 and 2D, with 1,4-benzenedicarboxylic acid as the ligand) [77]. This was likely because MIL-100(Fe) contains the Fe_3O cluster in its framework, thus the formed electron in the Fe_3O cluster could be effectively transferred from the metal center to the substrate. Previous studies have demonstrated a μ_3-O atom in the catalysts could promote the formation of a pronounced electronic delocalized state in the μ_3-O cluster unit, which could help electron transfer from the metal ion to the oxidant to form active species [83,84]. The results highlight the great potential to find more economical and sustainable MOFs

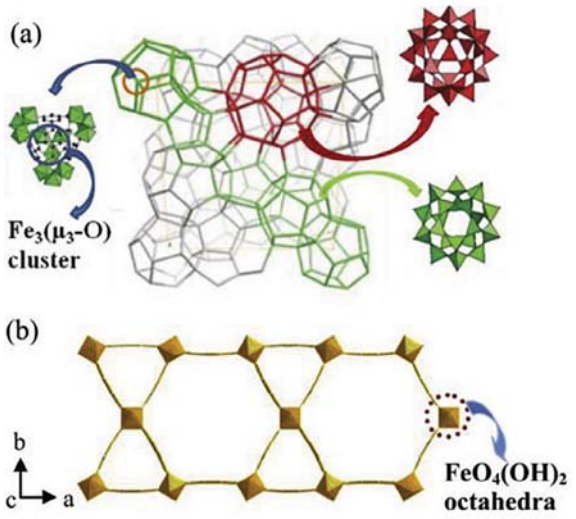

Fig. 1. (a) Topological view of MIL-100 with the MTN-type zeolitic architecture. (b) View of the structure of MIL-68 involving two types (hexagonal and trigonal) of channels running through the c-axis. Reproduced with permission from Ref. [77]. Copyright 2015 American Chemical Society.

for Fenton-like catalysis due to the fact that the structures of MOFs are highly tunable.

The efficiency of the MOF-catalyzed Fenton-like process can also be enhanced by introducing additional active sites to the catalyst. In a related work, Lv et al. [85] fabricated the novel Fe^{II}@MIL-100(Fe) Fenton-like catalyst (Fig. 2a) and studied its application in degrading methylene blue (MB) (detailed information of the pollutants mentioned in this review are provided in Table 1). After introducing Fe(II) species, Fe^{II}@MIL-100(Fe) was more positively charged and showed a lower adsorption ability for MB, which is believed to adversely affect the catalytic degradation process [28,86]. Nevertheless, Fe^{II}@MIL-100(Fe) presented a higher catalytic ability than MIL-100(Fe) catalysts [85]. The possible mechanism, as displayed in Fig. 2b, suggested the Fe(II) and Fe(III) ions in Fe^{II}@MIL-100(Fe) have synergistic effect on the generation of **.**OH radicals [85]. It is noteworthy that Fe(II) ions loaded on MIL-100 (Fe) might dissolve into the solution during the Fenton-like reaction. It was found that the concentration of leached Fe from Fe^{II}@-MIL-100(Fe) reached 7.1 mg/L, which may cause potential risks to the environment.

The efficiency of MOF-catalyzed Fenton-like processes can be enhanced by a combination of photoenergies (UV-light/visible light), which is currently an active research area. As a matter of fact, numerous research efforts have been devoted to photo-Fenton-like processes over the last two decades [87–89]. Recently, there has been more interest in developing new heterogeneous photo-Fenton-like processes [42,90,91]. It is well established that FeOOH could be a promising visible light photocatalyst due to its small band gap energy of 2.2–2.5 eV [92]. Unfortunately, the fast electron hole recombination rate on the photocatalyst largely limits the efficiency of the oxidation [92]. Some researchers have shown this can be overcome by reducing the particle size [93]. MOFs that contain a very small size of Fe(III) oxide clusters (5–8 nm) were therefore considered as visible light photocatalysts. In 2013, Laurier and co-workers [94] synthesized a new group MOFs containing Fe(III)-oxo clusters, and demonstrated their high photocatalytic efficiency for the degradation of rhodamine B (RhB). In the following works, several groups have found MIL-53(Fe) exhibited high photo-Fenton activity under visible light irradiation [95,96]. In a recent published work, the MIL-53(Fe)/H_2O_2/vis system showed significantly higher performance for the degradation of two PPCPs (clofibric acid and carbamazepine) than the MIL-53 (Fe)/H_2O_2, Fe(II)/H_2O_2 or TiO_2/vis systems [97]. It was concluded that the direct excitation of the iron-oxo cluster mainly contributes to the photo-Fenton activity of MIL-53(Fe). This viewpoint has also been proposed by several previous studies [98,99]. As shown in Fig. 3 [99], in the presence of H_2O_2 and visible light, the positive synergistic effects could contribute to the catalytic performance of MIL-53(Fe). Fe(III) ions on the surface of MIL-53(Fe) can catalyze the decomposition of H_2O_2 to produce **.**OH radicals via Fenton-like reactions (Eqs. (5) and (6)). On the other hand, H_2O_2 as an efficient scavenger could capture the photo-induced electrons in the excited MIL-53(Fe) to form **.**OH (Eqs. (7) and (8)).

$$\text{Fe(III) species} + H_2O_2 \rightarrow \text{Fe(II) species} + HO_2\cdot + H^+ \quad (5)$$

$$\text{Fe(II) species} + H_2O_2 \rightarrow \text{Fe(III) species} + \cdot OH + OH^- \quad (6)$$

$$\text{MIL-53(Fe)} + h\nu \rightarrow h^+ + e^- \quad (7)$$

$$H_2O_2 + e^-(\text{MIL-53(Fe)}) \rightarrow \cdot OH + OH^- \quad (8)$$

By composing MOFs with suitable materials, the physicochemical properties of catalysts can be further improved [100]. In 2014, the group of Wu and co-workers described the application of graphene oxide as a support for Fe-MIL-88B [101]. The RhB degradation efficiency by Fe-MIL-88B/graphene oxide under natural sunlight was significantly improved as compared to that by graphene oxide and Fe-MIL-88B separately. More recently, the group of Vu successfully synthesized a novel Fe-MIL-88B/graphene oxide composite by the solvothermal method [102]. They found that graphene oxide not only played a support role, but also contributed to

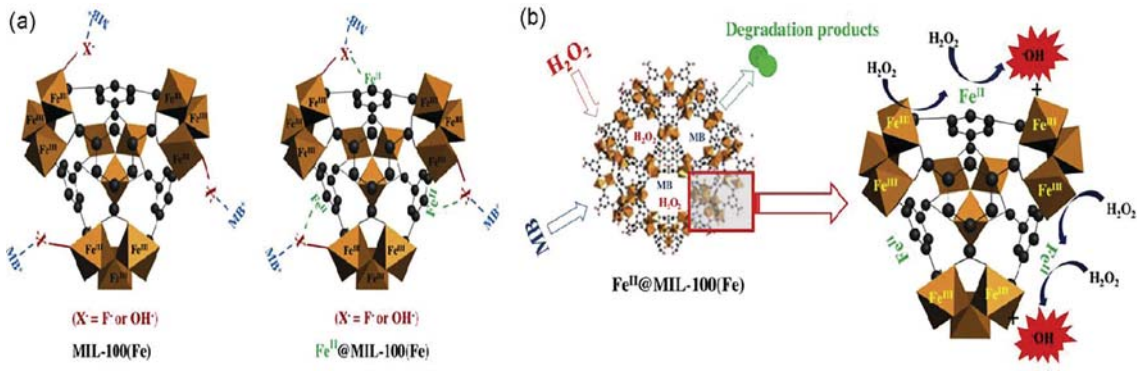

Fig. 2. (a) An electrostatic interaction between the dye MB and MOF-based materials, (b) proposed catalytic mechanism for the activation of H_2O_2 by Fe^{II}@MIL-100(Fe). Reproduced with permission from Ref. [85]. Copyright 2015 Elsevier.

Table 1
The detailed information of the mentioned pollutants in this review.

Pollutant	Abbreviation	Chemical formula	Molar mass g/mol	Structure
Acid orange 7	AO7	$C_{16}H_{11}N_2NaO_4S$	350.32	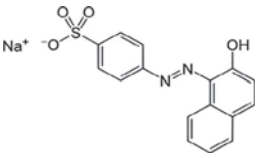
Bisphenol A	BPA	$C_{15}H_{16}O_2$	228.29	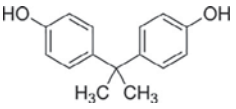
Carbamazepine	–	$C_{15}H_{12}N_2O$	236.27	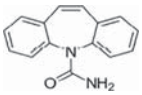
Clofibric acid	–	$C_{10}H_{11}ClO_3$	214.65	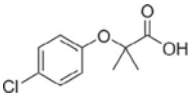
Congo red	CR	$C_{32}H_{22}N_6Na_2O_6S_2$	696.68	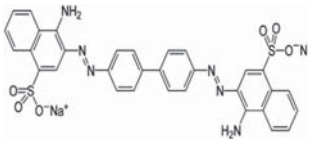
Diphenhydramine	DP	$C_{17}H_{21}NO$	255.36	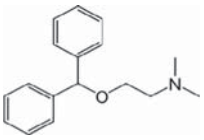
Methyl orange	MO	$C_{14}H_{14}N_3NaO_3S$	327.33	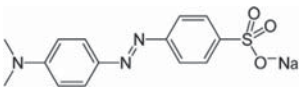
Methylene blue	MB	$C_{16}H_{18}ClN_3S$	319.85	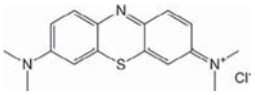
Rhodamine B	RhB	$C_{28}H_{31}ClN_2O_3$	479.02	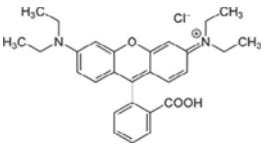
Phenol	–	C_6H_6O	94.11	
Phenytoin	PHT	$C_{15}H_{12}N_2O_2$	252.27	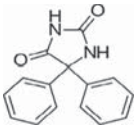

the formation of α-FeOOH by the interaction between the Fe(III) oxide species and hydroxyl/carboxylic groups in graphene oxide [103].

In practical applications for wastewater treatment, MOF-based catalysts are difficult to separate from the reaction solution for recycling due to their highly dispersive nature. The design of novel core-shell structures with Fe_3O_4 as the core and MOFs as the shell could be a feasible solution [104,105]. Fe_3O_4 nanoparticles have been extensively studied as heterogeneous Fenton-like catalysts due to their low toxicity and good magnetic properties [106]. However, Fe_3O_4 nanoparticles are highly susceptible to photodissolution [107]. Interestingly, the exciting radiation can be overcome

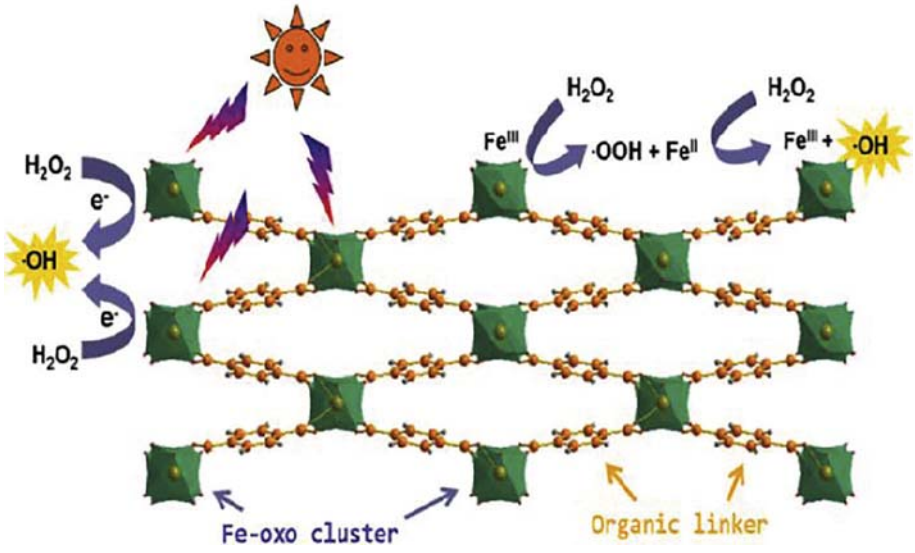

Fig. 3. Proposed mechanism for the activation of H_2O_2 by MIL-53(Fe) under visible light irradiation. Reproduced with permission from Ref. [99]. Copyright 2014 Elsevier.

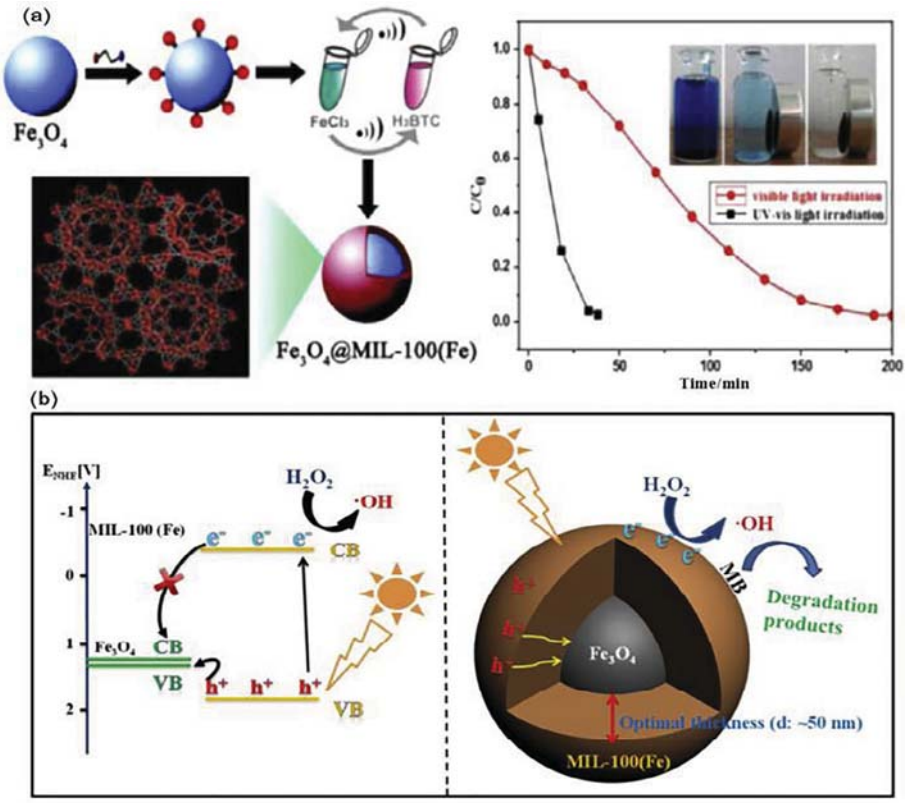

Fig. 4. (a) Fe_3O_4@MIL-100(Fe) first proposed for the activation of H_2O_2. Reproduced with permission from Ref. [108]. Copyright 2013 The Royal Society of Chemistry. (b) Illustration of the possible mechanism behind the enhanced photocatalytic ability of Fe_3O_4@MIL-100(Fe) with tunable thickness. Reproduced with permission from Ref. [109]. Copyright 2015 Wiley.

by using MOFs as the shell. In 2013, Zhang and co-workers [108] successfully fabricated the Fe_3O_4@MIL-100(Fe) catalyst through a simple method (Fig. 4a). The prepared catalyst can be easily separated and recycled without obvious loss of catalytic activity. More importantly, the MB degradation rate of the Fe_3O_4@MIL-100(Fe)/H_2O_2 photo-Fenton system was even higher than those of conventional C_3N_4 and TiO_2 photocatalysis systems. In the core-shell Fe_3O_4@MOFs/H_2O_2 photo-Fenton system, H_2O_2 acts as an electron acceptor and reacts with the photo-induced electrons on the MOFs, which suppresses the recombination of the photo-induced electron-hole pair (Fig. 4b) [109]. Further study revealed that the catalytic performance of the Fe_3O_4@MOFs/H_2O_2 photo-Fenton system is closely related to the thickness of the MOFs shell. Zhao et al. [109] examined the effect of the thickness of the shell (25–250 nm) on the photocatalytic ability of Fe_3O_4@MIL-100 and determined that the optimal thickness of the MOF shell is about 50 nm. It

was suggested that only a small number of electron-hole pairs would be generated when the thickness of the shell was too small; however, if the thickness of the shell was too large, the generated holes localized in the MOFs shell would not be able to access the Fe_3O_4 core [109,110]. Very recently, sulfonated Fe_3O_4@MIL-100 (Fe_3O_4 @MIL-100(Fe)-OSO_3H) has been synthesized by Moradi et al. [111] and proved to be an efficient Fenton-like catalyst. It was demonstrated that the sulfonate group of the MOF forms a new trap-state inside the band gap of Fe_3O_4@MIL-100(Fe), which promotes electron transfer between the sulfonate group and Fe_3O_4@MIL-100(Fe) at the interface.

3. Other single metal-based MOFs for heterogeneous Fenton-like catalysis

Apart from Fe-based MOFs, many other metals, such as Cu and Co, based MOFs have been synthesized and used as heterogeneous Fenton-like catalysts. Cu-based Fenton-like catalysts have attracted significant attention owing to the fact that the redox properties of copper are similar to iron [112–115]. In 2015, Lyu and co-workers [116] synthesized copper-doped mesoporous silica microspheres (Cu-MSMs) using a hydrothermal method. The characterization showed 0.91 wt% of the copper species was embedded in the framework of the MSMs by chemical binding of Cu-O-Si. The Cu-MSMs catalyzed Fenton process exhibited excellent performance for the degradation of phenytoin (PHT) and diphenhydramine (DP). The possible interaction process during the Fenton-like reaction is proposed in Fig. 5. In the first step, H_2O_2 was converted to **.**OH radical by the framework ≡Cu(I) in Cu-MSMs, and ≡Cu(I) was synchronously oxidized to ≡Cu(II). The generated **.**OH radical can then initiate the decomposition of PHT and DP. More importantly, the produced phenolic intermediates can be adsorbed on the surface of the Cu-MSMs, complexing with the framework ≡Cu(II) and forming ≡Cu-ligands, which can interact with H_2O_2 and facilitate the reduction of ≡Cu(II). As a result, ≡Cu-ligands accelerated the Cu (II)/Cu(I) cycles on the Cu-MSMs surface, leading to more efficient **.**OH generation for pharmaceutical degradation.

In addition to Cu(I) ions, Cu(II) ions were also utilized for MOF catalyst syntheses. For instance, a new five-coordinated copper-MOF, Cu_2(2,2′-bipyridine)$_2$ (pentafluorobenzoate)$_4$ (compound **1**), was hydrothermally synthesized by Han et al. in 2016 [117]. As seen from Fig. 6, each Cu(II) center in compound **1** is five coordinated to two nitrogen atoms and three oxygen atoms, presenting an approximately square-pyramidal coordination geometry. Compound **1** showed no catalytic activity for methyl orange (MO). However, in the presence of H_2O_2, about 85% of MO can be

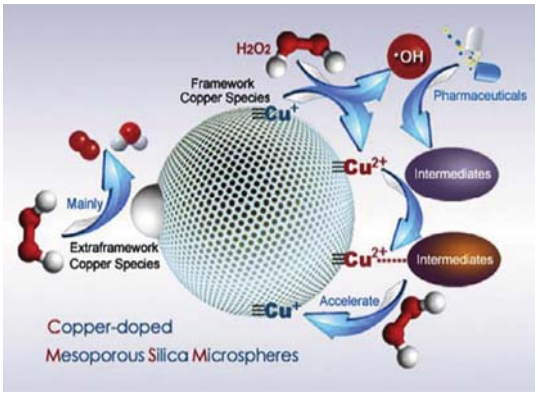

Fig. 5. A possible interaction process among the framework copper species of Cu-MSMs and H_2O_2. Reproduced with permission from Ref. [116]. Copyright 2015 Elsevier.

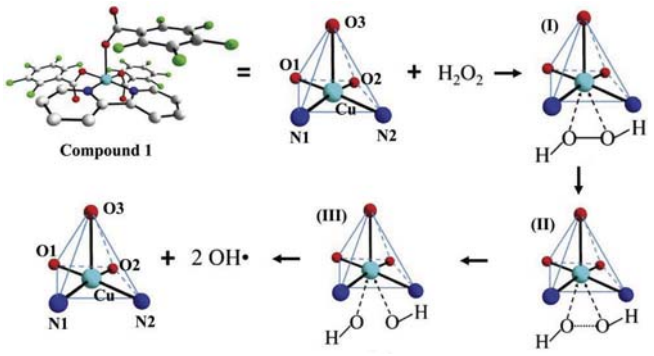

Fig. 6. The speculative mechanism of degrading MO. Reproduced with permission from Ref. [117]. Copyright 2016 The Royal Society of Chemistry.

removed from the solution in 15 min. The authors also discovered that the Fenton-like reaction did not change the structure of compound **1** and UV–vis radiation had no impact on the catalytic activity of this Fenton process. Based on the above findings, the probable mechanisms for MO degradation were proposed (Fig. 6). Firstly, **.**OH radicals can be generated by the Cu(II) catalytic decomposition of H_2O_2 through the Fenton-like process. Secondly, considering the molecular structure, the Cu(II) center of compound **1** trends to have six or seven-coordinated structure according to the valence bond theory; therefore, the five-coordinated Cu(II) center may coordinate to oxygen atoms from H_2O_2 molecules to form transition states I, II and III (Fig. 6). The Cu—O bonds in transition state III (oxygen atoms belonging to H_2O_2) would then be disconnected to produce **.**OH.

The cobalt ion based Fenton-like process has been investigated with H_2O_2, persulfate ($S_2O_8^{2-}$, PS) or peroxymonosulfate (HSO^{5-}, PMS) as the oxidant. In recent years, remarkable progress has been made in the synthesis of Co-based MOFs [118–122]. Bis-benzimidazole derivatives are often used as N-based ligands in the construction of Co-based MOFs, since their flexible nature allows them to bend and rotate freely with the metal centers [123]. On the other hand, aromatic dicarboxylates have proved to be excellent organic ligands due to their remarkable coordination ability, high structural stability and versatile coordination modes [120]. To take one step further, some research groups have focused their efforts on the fabrication of mixed-ligand MOFs. In a related report, three cobalt(II) based MOFs have been hydrothermally synthesized by the self-assembly of cobalt(II) nitrate with three flexible bis(benzimidazole) ligands and tetrabromoterephthalic acid (H_2tbta) (Fig. 7a) [119]. The degradation experiments showed compounds **3** and **4** (with 2D layer structures) can almost completely degrade congo red (CR), while compound **2** only presented a 77.3% removal, suggesting the structure of the MOFs plays an critical role in the catalytic activity of the catalysts. The results also indicated subtle differences in the organic ligand have a significant influence on the construction of the MOF structures. These findings are in agreement with the results of many other works. In a more recent study, a family of Co(II)-based MOFs has been synthesized using flexible bis(5,6-dimethylbenzimidazole) ligands [124]. It is observed that the spacers of the organic ligands and carboxylate anions have a great influence on the construction of different structures in the self-assembly process of bis(5,6-dimethylbenzimidazole) polymers. As shown in Fig. 7b, compound **5** features a 3-fold interpenetrating dia array with 4-connected networks; Compound **6** exhibits a 3D non-interpenetrated 3-connected framework; while compounds **7** and **8** display 2D networks. The discrepancy in the structures consequently led to the different Fenton-like catalytic activities. The 3D compounds (**5** and **6**) displayed much higher activities than the 2D compounds (**7** and **8**) for the activation of H_2O_2. When Compound

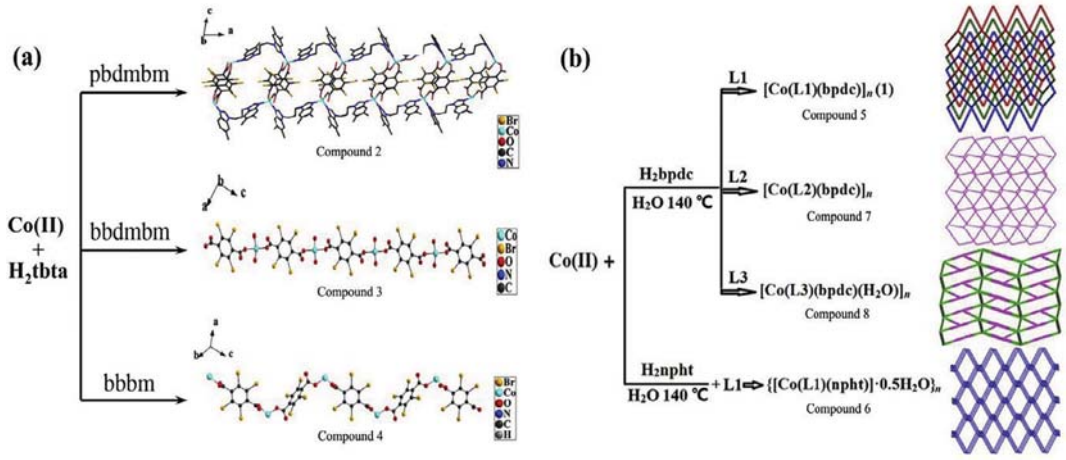

Fig. 7. (a) The synthetic routes and structures of compounds **2**, **3** and **4** based on flexible bis(benzimidazole) ligands and tetrabromoterephthalic acid [119]. Copyright 2015 Springer. (b) The synthetic routes and structures of compounds **5**, **6**, **7** and **8** based on flexible bis(5,6-dimethylbenzimidazole) ligands. Reproduced with permission from Ref. [124]. Copyright 2014 The Royal Society of Chemistry.

5 or **6** was used as the heterogeneous catalyst, the degradation efficiency of CR was 89 or 98% after 130 min, respectively. However, when compound **7** or **8** was introduced into the system, only about 56 or 52% of the dye was removed, respectively [124]. The different catalytic activities of the studied compounds may be due to the distinct coordination environments around the metal centers [122,125].

Some studies have been carried out on the comparison of catalytic activities of MOFs with the same organic ligands, but different metal ions. Recently, two new MOFs were obtained from copper acetates (Cu-A) or cobalt acetates (Co-A) and mixed ligands (siloxane dicarboxylic acid and 4,4-bipyridine) at room temperature [126]. The scanning electron microscope (SEM) images showed the synthesized Cu-A MOFs are quasi-spherical particles (spherulites) and the Co-A MOFs are cubic crystallites. Co-A was found have a smaller pore size, higher surface area and lower energy band gap. Consequently, Co-A showed much higher activity under natural sunlight irradiation as compared to the Cu catalyst. In a previous work, Yao et al. [127] discovered that using dicyandiamide as a C/N precursor, magnetic metal M (M = Fe, Co, Ni) nanocrystals could be embedded in nitrogen-doped carbon nanotubes (M@N-C) (Fig. 8a). The Fenton-like activity of M@N-C on the degradation of Acid Orange 7 (AO7) was examined using different oxidants (PMS, PS and H_2O_2). The results indicated that the catalytic activity followed the order Co@N-C > Fe@N-C > Ni@N-C. It was also found that PMS was the most suitable oxidant for these Fenton-like processes under neutral pH. The authors speculated that the high activation of PMS would be ascribed to the unique structural features in two aspects: the radical process and the non-radical process occur upon N doping in nitrogen-doped carbon nanotubes (Fig. 8b).

4. Heterobimetallic MOFs for heterogeneous Fenton-like catalysis

Pristine MOFs incorporated or doped with one or more other metal centers have received increasing attention in recent years, since the combination may enhance their particular activity [128–131].

Prussian blue (PB), a mixed-valence iron(III) hexacyanoferrate (II) compound, was accidentally discovered in 1704 by the Berlin artist Diesbach [132]. It is well known that PB converts into Fe $(OH)_3$ in alkaline solution [133], which limits its practical use in

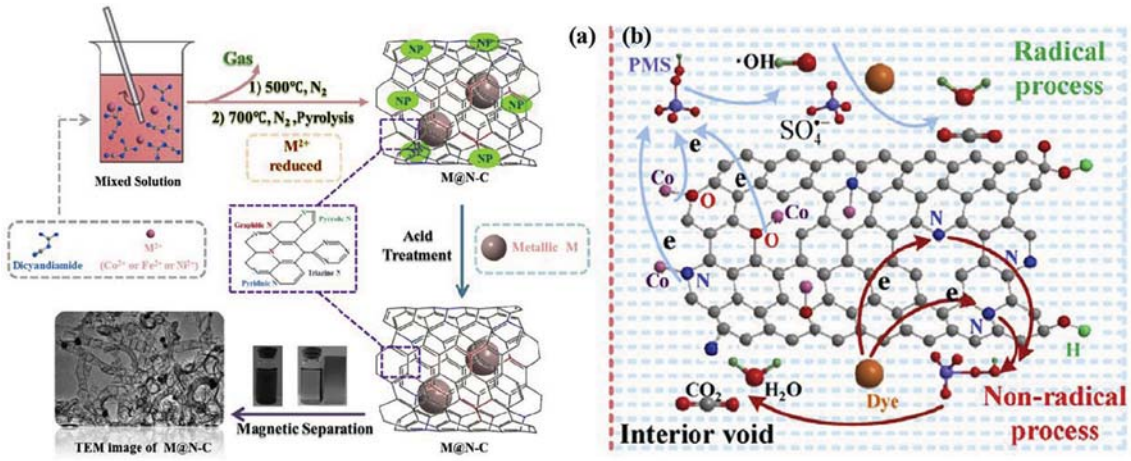

Fig. 8. (a) Schematic diagram for the syntheses of M@N-C catalysts (M = Ni, Fe, Co). (b) Mechanisms for dye degradation by the Co@N-C/PMS system. Reproduced with permission from Ref. [127]. Copyright 2016 Elsevier.

various catalytic reaction processes [134]. Wang and co-workers [135] developed another interesting application of PB analogues (PBAs), namely the catalytic removal of organic pollutants from solution. In 2015, they synthesized two kinds of Fe-Co PBAs as photo-Fenton catalysts [135]. The catalysts were constructed by Fe^{2+}/Fe^{3+} ions and octahedral $[Co(CN)_6]^{3-}$ anion groups, exhibiting cubic lattice structures. These two Fe-Co PBAs showed exceptionally high efficiencies for the decomposition of RhB at pH values from 3 to 8.5. The degradation capacity of the Fe(II)-Co PBA/H_2O_2/vis system was comparable to that of the homogeneous photo-Fenton process (Fe^{3+}/H_2O_2) under similar conditions. Apart from the conventional characterization techniques, Mössbauer spectroscopy was used to deeply explore the coordination environment and the oxidation state of the iron species in the Fe-Co PBAs during the photo-Fenton process. The entire photo-Fenton reaction mechanism of the Fe-Co PBAs is concluded in Fig. 9. In the first step of this process, the water molecules coordinated to iron sites were replaced by H_2O_2 molecules; the formed Fe(II)-peroxide complexes can then produce **.**OH radicals via Eq. (9). On the other hand, the Fe (III) ion in the catalysts could also be reduced by H_2O_2 at a slower rate to produce HOO**.** (Eq. (10)). In particular, $^1O_2$ produced from HOO**.** and **.**OH (Eqs. (11)–(14)) was proved to be directly involved in the degradation of RhB.

$$[Fe(CN)_5(H_2O)]^{3-} + H_2O_2 \rightarrow [Fe(CN)_5(HO)_2]^{3-} + H_2O \rightarrow [Fe(CN)_5(H_2O)]^{2-} + \mathbf{.}OH + OH^- \quad (9)$$

$$[Fe(CN)_5(H_2O)]^{2-} + H_2O_2 \rightarrow [Fe(CN)_5(HO)_2]^{2-} + H_2O \rightarrow [Fe(CN)_5(H_2O)]^{3-} + HOO\mathbf{.} + H^+ \quad (10)$$

$$HOO\mathbf{.} \rightarrow H^+ + O_2\cdot^- \quad (11)$$

$$O_2\cdot^- + \mathbf{.}OH \rightarrow {}^1O_2 + OH^- \quad (12)$$

$$HOO\mathbf{.} + O_2\cdot^- \rightarrow {}^1O_2 + HO_2^- \quad (13)$$

$$HOO\mathbf{.} + HOO\mathbf{.} \rightarrow {}^1O_2 + H_2O_2 \quad (14)$$

In the following year, this group reported that hydrazine (Hz) could significantly promote the degradation performance of the Fe-Co PBA-based Fenton-like process [136]. Hz increased the activity of Fe(III)-Co PBA for bisphenol A (BPA) degradation by over two orders of magnitude at pH = 4.0. Two mechanisms could account for this dramatic enhancement in BPA degradation. Firstly, the Hz coordinated iron sites in the catalyst were identified to be more active than the original ones. Secondly, the addition of Hz could enhance the dissolution of Fe(III)-Co PBA, which largely increased the reaction rate. In the same year, this group has successfully synthesized porous $Fe_xCo_{3-x}O_4$ nanocages based on Fe-Co PBAs [137]. It was reported that the CN— group in the Fe-Co PBAs can be removed by heating at 500 °C for 1 h. The obtained $Fe_xCo_{3-x}O_4$ nanocages showed much higher catalytic activity compared with Co_3O_4 and Fe_3O_4, which was believed to be mainly due to the presence of octahedral (B-site) Co(II) ions on the catalyst surface. B-site Co(II) ions could provide electrons and lead to an increase of Co(III) ions at the B-site. B-site Co(III) ions would then accept electrons from the system to keep the charge balance on the catalyst surface, which suggested Co(II)-Co(III)-Co(II) redox cycles were involved in the catalytic oxidation reaction [138].

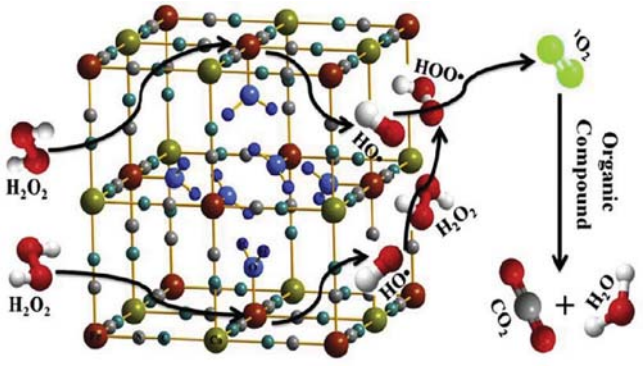

Fig. 9. Proposed photo-Fenton reaction mechanism over the cubic lattice structure of Fe-Co PBAs. Reproduced with permission from Ref. [135]. Copyright 2015 Elsevier.

In 2005, Ferey et al. [139] reported the discovery of the mesoporous Cr-MIL-101 which exhibited a high specific surface area, incredibly larger pore size (2.9–3.4 nm) and significantly high hydro- and thermal stability. Following this work, extensive attempts have been made to incorporate metal nanoparticles into the Cr-MIL-101 framework to produce new types of catalysts. In 2014, Vu's group published the incorporation of Fe atoms (by an amount of ca. 25% of the Cr atoms) into Cr-MIL-101 by a conventional solvothermal method [140]. In this case, Fe-Cr-MIL-101 showed high photo-Fenton activity and high stability, whereas Cr-MIL-101 exhibited almost no Fenton catalytic activities. This result suggested that the Fe(III) sites in Fe-Cr-MIL-101 are mainly responsible for the decomposition of H_2O_2. In the following year, Qin and co-workers [141] present an organic acid (citric acid, CA) cooperative strategy to assemble Fe-C oxides on the coordinatively unsaturated Cr sites of MIL-101 (Cr). This method can prevent the nanoparticles from aggregating on the outer surface of host matrix. Different from conventional solution impregnation, the addition of CA can remarkably enhance the binding between metal ions and the secondary building units of the MOFs, which is very useful in metal loading control (Fig. 10a). The property dependence of MOF materials on the photo-Fenton catalytic activity was also investigated by comparing Fe^{3+}-CA/MIL-101(Cr) with Fe^{3+}-CA/MIL-53(Cr) in this report. The results revealed that the former system exhibited 10 times more activity than the later one in terms of decoloration and TOC removal, which suggested the structure and properties of the support had a significant effect on the activity of the catalysts for the decomposition of H_2O_2. As illustrated in Fig. 10b, the grafting of Fe-C oxide nanoparticles dispersed on the outer surface and into cavities of MIL-53 led to a loss of activity due to detrimental interactions between the nanoparticles and support [142,143]. The metal-oxo cluster excitation and ligand-to-metal charge transfer were known to play an important role in the photocatalytic properties of MOFs [94,144,145]. In this regard, it was reasonable to believe that the exceptionable catalytic activity of Fe^{3+}-CA/MIL-101(Cr) was derived from the direct excitation of the Cr-oxo cluster and interfacial photo-generated charge transfer between [Fe-O-C] sites and Cr nodes [144].

To improve the catalytic performances of MOFs, some researchers have focused their efforts on the introduction of noble-metal nanoparticles into such materials. Several approaches, including incipient wetness impregnation, colloidal synthesis and chemical vapor deposition, have been studied for the fabrication of noble-metal doped MOF nanocomposites [144,146–149]. However, many of these techniques result in high energy consumption or insufficient interfacial contact between the noble-metal nanoparticles and the MOFs [150]. In 2015, Liang et al. [150] successfully fabricated Pd@MIL-100(Fe) using a facile alcohol reduction method at 90 °C. It was demonstrated that Pd atoms on the surface of Pd@MIL-100(Fe) can reduce the recombination of photogenerated electron-hole pairs and thereby improve the photocatalytic performance of the original-MIL-100(Fe). In the same year, a series of M@MIL-100(Fe) catalysts (M = Au, Pd, and Pt) were synthesized by the same group, fabricated though a photodeposition technique

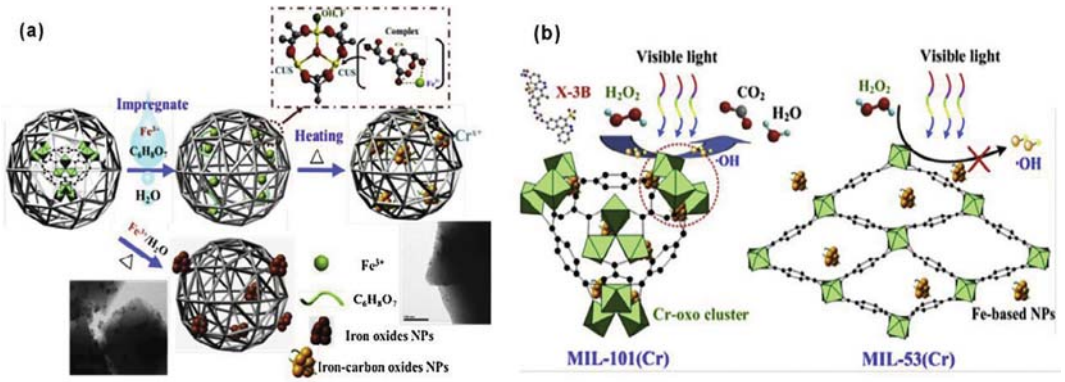

Fig. 10. (a) Preparation of MIL-101(Cr) supporting Fe–carbon oxides through a cooperative organic-acid-directed method with thermal treatment. Without CA, most Fe_2O_3 aggregated on the outer surface of the MOF due to external diffusion of the precursor during the heating process. (b) Schematic diagram of MIL-101(Cr) and MIL-53(Cr) supported catalysts for the activation of H_2O_2 in the catalytic oxidation. Reproduced with permission from Ref. [141]. Copyright 2015 Elsevier.

at room temperature [151]. The photocatalytic activities of the prepared catalysts were found to be in the following order: Pt@MIL-100(Fe) > Pd@MIL-100(Fe) > Au@MIL-100(Fe) > MIL-100(Fe). The higher photoactivity of M@MIL-100(Fe) (M = Au, Pd, and Pt) can be attributed to the synergistic effect between the metal nanoparticles and MIL-100(Fe), the efficient charge-carrier separation and enhanced visible-light absorption [152,153]. In the both cases, **·**OH radicals can be generated though the decomposition of H_2O on the photogenerated holes and the reactions of H_2O_2 with photogenerated electrons/Fe(III)-O clusters, as shown in Fig. 11 [151].

The utilization of MOF materials as precursors or templates to produce porous Fenton-like catalysts has also been demonstrated [154,155]. In a previous work, Bao and co-workers [156] presented a solvothermal method to synthesize $CuFe_2O_4$/Cu@C composite materials derived from 1,3,5-benzenetricarboxylic ([Cu/Fe]-BTC) MOFs. The as-synthesized $CuFe_2O_4$/Cu@C composite showed a higher catalytic activity than Fe_3O_4@C, which confirmed the importance of copper doping in the catalyst [156]. In a recent study, series of graphene-encapsulated transition-metal nitrides ($Fe_xMn_{6-x}Co_4$-N@C; $0 < x < 6$) with well-controlled morphologies were

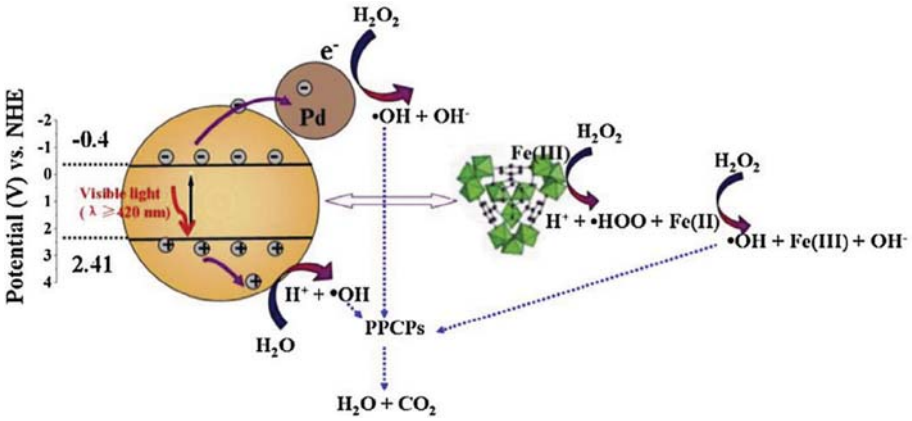

Fig. 11. Proposed mechanism for the photocatalytic degradation of PPCPs over Pd@MIL-100(Fe) under visible light irradiation. Reproduced with permission from Ref. [151]. Copyright 2015 Elsevier.

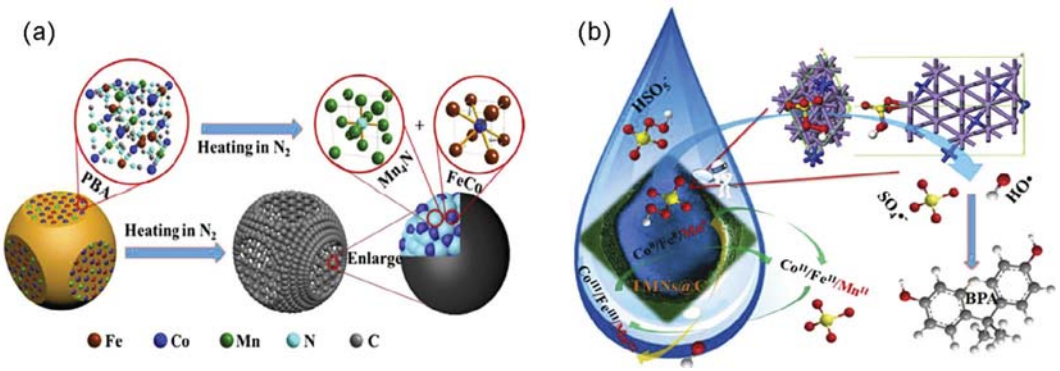

Fig. 12. (a) Preparation route and model of the graphene encapsulated TMNs ($FexMn_{6-x}Co_4$–N@C) with well controlled morphology. (b) Proposed mechanism for PMS activation over $FexMn_{6-x}Co_4$–N@C nanodices. Reproduced with permission from Ref. [157]. Copyright 2015 American Chemical Society.

synthesized through the thermal decomposition of MOFs (Mn_y-Fe_{1-y}-Co PBAs) at 650 °C in a N_2 atmosphere (Fig. 12a) [157]. Under such conditions, the CN— group of the PBAs serve as nitrogen and carbon sources to form nitrogen doped graphene layers [158–161]. Meanwhile, Co and Fe atoms form a Fe-Co alloy, while Mn atoms form Mn_4N nanocrystals inside the catalysts. The Fenton-like degradation of BPA showed $Fe_xMn_{6-x}Co_4$-N@C are highly efficient catalysts for PMS activation, which was mainly attributed to the coexistence of Fe, Mn, and Co species in the catalysts [157]. As illustrated in Fig. 12b, $\equiv Mn^0/Fe^0/Co^0$ in $Fe_xMn_{6-x}Co_4$-N@C could activate PMS to produce **.**OH and $SO_4^{\cdot-}$ radicals whilst being oxidized to $\equiv Mn^{2+}/Fe^{2+}/Co^{2+}$ and $\equiv Mn^{3+}/Fe^{3+}/Co^{3+}$. On the other hand, the formed $\equiv Mn^{3+}/Fe^{3+}/Co^{3+}$ could be further reduced to $\equiv Mn^{2+}/Fe^{2+}/Co^{2+}$ by PMS, thus making the reaction proceed cyclically until the PMS was completely consumed [162–164]. Additionally, the authors found that am increase in the Mn content could largely enhance the catalytic performance, suggested that Mn_4N can facilitate electron transfer for PMS activation.

5. The effects of pH on the performance of MOFs-based Fenton-like catalysis

It is very necessary to understand the effect of the initial pH on the catalytic activity of MOF-based catalysts since actual wastewater always has variable pH values [165–169]. Several works have suggested that MOF-based Fenton-like catalysis could work over a wide pH range [85,99,135,156,170]. For example, Ai et al. [99] reported that H_2O_2 can be decomposed on the reactive metals sites of the MIL-53(Fe) catalyst over a wide pH range, from 3.0 to 9.0. However, it is worth noticing that the degradation rate of RhB decreased with the increase of the initial pH values. A similar result was reported in a recent study [97], in which the degradation performance of MIL-53(Fe)/H_2O_2/vis was found to be closely dependent on the initial solution pH. The apparent rate constant of carbamazepine degradation at pH 3 is over 6 times faster than that at pH 7. High pollutant removal efficiency at low pH values can be explained by the fact that Fenton/Fenton-like reactions between H_2O_2 and Fe in the catalysts preferred acidic conditions [171]. Besides, for some catalysts (e.g., Fe_3O_4/C/Cu), a higher concentration of metal ions would dissolve at lower pH values, enhancing the generation of **.**OH radicals though homogeneous Fenton/Fenton-like reactions [170]. It is also reported that an increase of the pH from acidic (pH 3.0) to neutral (pH 6.5) has limited impact on the catalytic performance of Fe_3O_4@MIL-100 in the photo-Fenton process [109]. A possible explanation for this observation is that the reaction between photoinduced electrons and H_2O_2 takes an important part in **.**OH generation. The combination of Fe and other metals (Cu/Co) allows the Fenton-like process to be conducted over an even broader pH range. For example, Bao et al. [156] reported that nearly complete removal of MB was achieved in 15 min at pH values of 3.02, 5.12 and 8.14 by a $CuFe_2O_4$/Cu@C catalyzed Fenton-like reaction, but the removal efficiency would dramatically decrease as the pH values was further increased to 10.0 or higher. This is because in alkali media, H_2O_2 loses its oxidizing ability due to its decomposition to H_2O and O_2 [111,172]. Based on the results obtained from lab-scale experiments (Table 2), it is reasonable to conclude that MOF-based Fenton-like catalysis is generally effective in the pH range 3.0–6.0. It is well known that the traditional homogeneous Fenton process is required to be operated in the pH range 2.8–3.5 [7], which is the primary drawback of this technique. Promising results have been obtained using MOF-based Fenton-like catalysis, showing that these technologies may help to solve this problem in the near future.

6. Stability and reusability of MOF-based Fenton-like catalysts

The stability of MOF-based catalysts is a key issue that should be considered, especially from the view of actual applications. Firstly, it is important to know whether MOF-based Fenton-like catalysts could maintain their initial structures during the oxidation process. Gao et al. [97] studied the Fourier transform infrared spectroscopy (FTIR) spectra and X-ray diffraction (XRD) patterns of samples before and after the reactions, finding that the crystal and chemical structures of MIL-53(Fe) are almost unchanged after four cycles. Similar results were published in many other works [81,85,99,135], suggesting that the Fenton-like process has little impact on the main structure of the MOFs catalysts. On the other hand, leaching of metal ions from the MOFs catalysts was monitored to get a better understanding of sample stability (Table 2). It is well known that traditional heterogeneous Fenton-like catalysts, such as iron oxides, would undoubtedly result in leaching of metal ions, giving rise to high risks to human beings [127]. Due to their special structure, MOF-based Fenton-like catalysts generally exhibited higher stability than traditional heterogeneous Fenton-like catalysts. For instance, Lv et al. [85] found the leaching of Fe from MIL-100(Fe) after 240 min reaction was only 14% of the Fe_2O_3 catalyst. In another study, the MIL-100(Fe) layer was found to be able to reduce the leaching of Fe from the Fe_3O_4 core [109]. For Fe_3O_4@MIL-100, with 10, 20 or 40 layers of MIL-100, the iron leaching was 2.93, 0.86, 0.41 mg/L after a reaction time of 3 h,

Table 2
The suitable operation pH, reusability and leaching ions of some studied MOF Fenton-like catalysts.

Catalyst	Suitable pH	Reusability	Leached ions	Refs.
MIL-100(Fe): 2500 mg/L	NA	No obvious loss of catalytic activity after 3 cycles.	No detectable Fe	[77]
MIL-100(Fe): 1000 mg/L	3.0–8.0	NA	Fe: 2.2 mg/L	[85]
MIL-88B-Fe: 100 mg/L	4.0–5.0	Catalytic performance almost unchanged after 4 recycles.	Fe: 0.82 mg/L	[82]
MIL-53(Fe): 100 mg/L	3.0–5.0	4 successive runs without obvious loss of activity.	NA	[97]
MIL-53(Fe): 400 mg/L	3.0–9.0.	Catalytic performance almost unchanged after 3 recycles.	NA	[99]
Fe^{II}@MIL-100(Fe): 1000 mg/L	3.0–8.0	NA	Fe: 7.1 mg/L	[85]
Fe-bpydc: 10 mg/L	3.0–6.0	Catalytic activity decreased after 2nd and 3rd runs.	NA	[81]
Fe_3O_4@MIL-100: 100 mg/L	3.0–6.5	4 successive runs without obvious loss of activity.	Fe: 0.86 mg/L	[109]
Fe–Cr-MIL-101: 300 mg/L	3.2–5.5.	Catalytic activity almost unchanged after 3 recycles.	Fe: 1.5 mg/L	[140]
Fe^{3+}-CA/MIL-101: 100 mg/L	NA	4 successive runs without obvious loss of activity.	Fe < 0.08 mg/L Cr < 0.01 mg/L	[141]
Co@N-C: 20 mg/L	NA	Catalytic activities slightly decreased after 5 recycles.	No detectable Co	[127]
$CuFe_2O_4$/Cu@C: 500 mg/L	3.02–8.14	Retained its original activity after 10 runs.	NA	[156]
Fe_3O_4/C/Cu: 500 mg/L	3.0–9.0	5 successive runs without obvious loss of activity.	NA	[170]
Fe^{III}–Co PBA: 200 mg/L	3.0–8.5	Good performance in the subsequent 4-cycle runs.	Fe < 0.15 mg/L Co < 0.15 mg/L	[135]
$Fe_{0.8}Co_{2.2}O_4$: 100 mg/L	NA	Good performance even after 4-cycle runs.	Fe: 0.11 mg/L Co: 0.36 mg/L	[137]
Pd@MIL-100 (Fe): 125 mg/L	4.0–6.0	No obvious loss of catalytic activity after 4 cycles.	Almost no ions leached.	[151]

respectively. According to the scientific results, the amount of leached metals was largely dependant on the chemical structure of the catalysts. For example, Lv et al. [85] found that the leached Fe from Fe^{II}@MIL-100(Fe) reached 7.1 mg/L, however, other researchers reported the leached Fe from $Fe_xCo_{3-x}O_4$ nanocages [137] and their predecessor Fe-Co PBA [135] was only about 0.1 mg/L. The addition of a chelating agent, such as an organic acid, can remarkably enhance the stability of the MOF-based catalysts. As reported by Qin et al. [141], the leached Fe from Fe^{3+}-CA/MIL-101(Cr) was below 0.08 mg/L, which was much lower than that leached from Fe-MIL-101(Cr) (1.5 mg/L) [140]. It was believed that a stable bridge from CA molecules was established between Fe^{3+} ions and the secondary building units of the MOF, which protected the Fe^{3+} ions from leaching into the solution [141]. As shown in Table 2, the concentrations of leached metals in most cases are below the environmental standard (2 mg/L) imposed by the European Union [82]. Interestingly, the catalytic performance of the leached metal iron ions was investigated in a recent published work [82]. In the experiment, the catalyst (MIL-88B-Fe) was dispersed into a phenol solution by sonication, and then the suspension was stirred for 30 min. After MIL-88B-Fe was removed by filtration, H_2O_2 solution was added to the solution to initiate the homogeneous catalysis. It was found phenol degradation catalyzed by the leached iron ions was negligible. The results suggested that the catalytic activity of MIL-88B-Fe was dominated by heterogeneous catalysis rather than homogeneous catalysis resulting from the leached iron ions. This result is consistent with the findings by Hu et al. [173], who proposed that Fenton-like oxidation mainly occurs at the solid-liquid interface.

From the view of long-term industrial applications, the reusability of MOF-based catalysts is another prominent issue to be considered. In most cases, as summarized in Table 2, the prepared MOFs catalysts were very stable and could be used for repeated treatment of organic pollutants. The catalytic performance of the MIL-53(Fe) [97,99], Fe-Cr-MiL-101 [140], Fe_3O_4@-MIL-100 [109], $CuFe_2O_4$/Cu@C [156] and MOF(2Fe/Co)/CA [174] catalysts could be maintained at the level of a fresh sample after three or more recycles. On the other hand, there are also observations that the catalytic activities of MOFs catalysts decrease with increasing multiple use of the catalysts, mainly due to blockage of the active sites by degradation intermediates [81,127,137].

7. Concluding remarks and prospects

As has been stated in this review, the application of MOF based catalysts represents a promising alternative to homogeneous Fenton processes as well as to the use of conventional catalysts in Fenton-like oxidation. The high specific area, large pore volume and chemical tenability of MOF materials make them attractive for that purpose. Particularly promising are the most recent results reported with heterobimetallic MOF catalysts, which allow high rates of homogeneous Fenton-like processes to be achieved. The conclusions derived from the various literature sources can be stated as follows:

1. MOF materials with fixed metal centers are able to catalyze H_2O_2 to generate **.**OH radicals over a wide pH range, even in neutral/alkaline conditions under heterogeneous reaction conditions.
2. Amongst various preparation methods, the solvothermal method has been used as a common technique for the production of MOFs catalysts. Among the various MOFs, iron-based MIL materials have gained particular attention in homogeneous Fenton-like catalysis.
3. Changes in flexibility, spacer length and symmetry of the ligands can result in a wide range of MOF materials bearing diverse architectures and functions, and their chemical structures are closely related to the catalytic performance of the homogeneous Fenton-like catalysis.
4. The efficiency of MOF catalyzed Fenton-like catalysis can be enhanced by combining this process with photoenergies or by introducing additional activity sites, such as noble-metal nanoparticles, into the MOF materials.
5. There is growing interest in using heterobimetallic MOFs for heterogeneous Fenton-like catalysis. The incorporated or doped new metals can effectively enhance the catalytic performance of the pristine MOFs.
6. Suitable recycling times and water stability are essential for actual working place considerations. Under tested conditions, most MOF catalysts were shown to be stable, with limited metal ion leaching. However, the capacity of some highly efficient MOFs would gradually decrease in the cycling runs mainly due to blockage of the active sites by degradation intermediates.

Note, research in this field is still at an early stage. Many improvements are required before the technology can be scaled up to bench and pilot plant levels.

1. Their potential application is still limited by a number of shortcomings, such as aggregation, consequent loss of dispersibility and iron leaching. Moreover, they can be entrained during supernatant discharge. Their immobilization onto a support or a magnetic core could be potential solutions; however, the attempts reported so far showed that metal leaching cannot be completely avoided. Therefore, there is room for considerable improvements in this field.
2. Another important consideration is that most studies have been conducted with simulated wastewater; few studies have been conducted with actual polluted water. Recall that huge differences could be obtained between pollutant removal efficiencies in simulated wastewater and actual polluted wastewater. A good example can be found in a recent study by Gao and co-workers [97] in which the Fenton-like process using MIL-53(Fe) yielded more than 94% of removal in river water and 71% of removal in municipal wastewater. Therefore, significant effort is required to assess these technologies for use with real wastewater.
3. Most studies to date have been conducted at the lab-scale using small reactors. To meet commercial demonstrations, more attention should be devoted in the future to investigating their economic and operational feasibility, and any problems arising from the scale-up.
4. Many issues still need to be investigated at the lab-scale, especially in terms of obtaining a fundamental understanding of these processes. For example, the metal-ligand complexes-associated mechanism needs further in-depth study, these results are encouraging for the rational design of new MOF Fenton-like catalysts and the application of MOF Fenton-like processes under neutral conditions.
5. Systematic research is still required to examine the stability of MOF catalysts for a wider range of operational conditions to avoid the leaching of these metals into the reaction solution.
6. The removal of pollutants in MOF systems are very efficient, while the mineralization is somewhat lower, therefore, in the treatment of actual wastewater, combining this technology with other complementary treatments, such as conventional bio-oxidation, could become an active research area.

Acknowledgements

This study was financially supported by the Program for the National Natural Science Foundation of China (51579098,

51521006, 51378190, 51408206), the National Program for Support of Top-Notch Young Professionals of China (2014), the Program for Changjiang Scholars and Innovative Research Team in the University (IRT-13R17), the Program for New Century Excellent Talents in the University (NCET-13-0186), Hunan Provincial Innovation Foundation for Postgraduate (CX2017B098) and Hunan Provincial Science and Technology Plan Project (No. 2016RS3026).

References

[1] C.J. Vörösmarty, P.B. McIntyre, M.O. Gessner, D. Dudgeon, A. Prusevich, P. Green, S. Glidden, S.E. Bunn, C.A. Sullivan, C. Reidy Liermann, Nature 467 (2010) 555.
[2] G. Zeng, M. Chen, Z. Zeng, Nature 499 (2013) 154.
[3] P. Xu, G.M. Zeng, D.L. Huang, C.L. Feng, S. Hu, M.H. Zhao, C. Lai, Z. Wei, C. Huang, G.X. Xie, Sci. Total Environ. 424 (2012) 1–10.
[4] I. Ali, Chem. Rev. 112 (2012) 5073–5091.
[5] C.A. Martínez-Huitle, M.A. Rodrigo, I. Sirés, O. Scialdone, Chem. Rev. 115 (2015) 13362–13407.
[6] M. Cheng, G. Zeng, D. Huang, C. Lai, Z. Wei, N. Li, P. Xu, C. Zhang, Y. Zhu, X. He, Appl. Microbiol. Biotechnol. 99 (2015) 5247–5256.
[7] E. Brillas, I. Sirés, M.A. Oturan, Chem. Rev. 109 (2009) 6570–6631.
[8] J.-L. Gong, B. Wang, G.-M. Zeng, C.-P. Yang, C.-G. Niu, Q.-Y. Niu, W.-J. Zhou, Y. Liang, J. Hazard. Mater. 164 (2009) 1517–1522.
[9] K. Vellingiri, L. Philip, K.-H. Kim, Coord. Chem. Rev. 353 (2017) 159–179.
[10] M. Cheng, G. Zeng, D. Huang, C. Yang, C. Lai, C. Zhang, Y. Liu, Crit. Rev. Biotechnol. (2017) 1–14.
[11] M. Cheng, G. Zeng, D. Huang, C. Lai, Y. Liu, P. Xu, C. Zhang, J. Wan, L. Hu, W. Xiong, C. Zhou, Chem. Eng. J. 327 (2017) 686–693.
[12] C. Yang, H. Chen, G. Zeng, G. Yu, S. Luo, Biotechnol. Adv. 28 (2010) 531–540.
[13] J. Ren, X. Dyosiba, N.M. Musyoka, H.W. Langmi, M. Mathe, S. Liao, Coord. Chem. Rev. 352 (2017) 187–219.
[14] M. Cheng, G. Zeng, D. Huang, C. Lai, Y. Liu, C. Zhang, R. Wang, L. Qin, W. Xue, B. Song, S. Ye, H. Yi, J. Colloid Interface Sci. 515 (2018) 232–239.
[15] C. Zhou, C. Lai, P. Xu, G. Zeng, D. Huang, C. Zhang, M. Cheng, L. Hu, J. Wan, Y. Liu, W. Xiong, Y. Deng, M. Wen, ACS Sustainable Chem. Eng. 6 (2018) 4174–4184.
[16] M. Cheng, G. Zeng, D. Huang, C. Lai, C. Zhang, Y. Liu, Chem. Eng. J. 314 (2017) 98–113.
[17] M. Cheng, G. Zeng, D. Huang, C. Lai, P. Xu, C. Zhang, Y. Liu, Chem. Eng. J. 284 (2016) 582–598.
[18] J.J. Pignatello, E. Oliveros, A. MacKay, Crit. Rev. Environ. Sci. Technol. 36 (2006) 1–84.
[19] E. Neyens, J. Baeyens, J. Hazard. Mater. 98 (2003) 33–50.
[20] M.I. Litter, M. Slodowicz, J. Adv. Oxid. Technol. 20 (2017) 19.
[21] D. Huang, C. Hu, G. Zeng, M. Cheng, P. Xu, X. Gong, R. Wang, W. Xue, Sci. Total Environ. 574 (2017) 1599–1610.
[22] F. Haber, J. Weiss, in: Proceedings of the Royal Society of London A: Mathematical, Physical and Engineering Sciences, The Royal Society, 1934, pp. 332–351.
[23] J. Hoigné, H. Bader, Water Res. 17 (1983) 185–194.
[24] A.D. Bokare, W. Choi, J. Hazard. Mater. 275 (2014) 121–135.
[25] G. Ren, M. Zhou, M. Liu, L. Ma, H. Yang, Chem. Eng. J. 298 (2016) 55–67.
[26] R. Davarnejad, J. Azizi, J. Environ. Chem. Eng. 4 (2016) 2342–2349.
[27] T.X.H. Le, M. Bechelany, S. Lacour, N. Oturan, M.A. Oturan, M. Cretin, Carbon 94 (2015) 1003–1011.
[28] X. Gong, D. Huang, Y. Liu, G. Zeng, R. Wang, J. Wan, C. Zhang, M. Cheng, X. Qin, W. Xue, Environ. Sci. Technol. 51 (2017) 11308–11316.
[29] C. Hu, D. Huang, G. Zeng, M. Cheng, X. Gong, R. Wang, W. Xue, Z. Hu, Y. Liu, Chem. Eng. J. 338 (2018) 432–439.
[30] Y. Ju, Y. Yu, X. Wang, M. Xiang, L. Li, D. Deng, D.D. Dionysiou, J. Hazard. Mater. 323 (2017) 611–620.
[31] J.A. Khan, X. He, H.M. Khan, N.S. Shah, D.D. Dionysiou, Chem. Eng. J. 218 (2013) 376–383.
[32] Z. Qiang, J.-H. Chang, C.-P. Huang, Water Res. 37 (2003) 1308–1319.
[33] H. Katsumata, S. Kaneco, T. Suzuki, K. Ohta, Y. Yobiko, Chem. Eng. J. 108 (2005) 269–276.
[34] B.C. Faust, J. Hoigné, Atmos. Environ. Part A 24 (1990) 79–89.
[35] F. Duarte, V. Morais, F. Maldonado-Hódar, L.M. Madeira, Chem. Eng. J. 232 (2013) 34–41.
[36] J. Deng, J. Jiang, Y. Zhang, X. Lin, C. Du, Y. Xiong, Appl. Catal. B: Environ. 84 (2008) 468–473.
[37] S. Ammar, M.A. Oturan, L. Labiadh, A. Guersalli, R. Abdelhedi, N. Oturan, E. Brillas, Water Res. 74 (2015) 77–87.
[38] M. Cheng, G. Zeng, D. Huang, C. Lai, P. Xu, C. Zhang, Y. Liu, J. Wan, X. Gong, Y. Zhu, J. Hazard. Mater. 312 (2016) 184–191.
[39] D. Huang, W. Xue, G. Zeng, J. Wan, G. Chen, C. Huang, C. Zhang, M. Cheng, P. Xu, Water Res. 106 (2016) 15–25.
[40] S.R. Pouran, A.A.A. Raman, W.M.A.W. Daud, J. Clean. Prod. 64 (2014) 24–35.
[41] E. Garrido-Ramírez, B. Theng, M. Mora, Appl. Clay Sci. 47 (2010) 182–192.
[42] J. Herney-Ramirez, M.A. Vicente, L.M. Madeira, Appl. Catal. B: Environ. 98 (2010) 10–26.
[43] M. Munoz, Z.M. De Pedro, J.A. Casas, J.J. Rodriguez, Appl. Catal. B: Environ. 176 (2015) 249–265.
[44] L. Hou, L. Wang, S. Royer, H. Zhang, J. Hazard. Mater. 302 (2016) 458–467.
[45] H. Kitagawa, H. Ohtsu, M. Kawano, Angew. Chem. Int. Ed. 52 (2013) 12395–12399.
[46] J. Park, D. Feng, H.-C. Zhou, J. Am. Chem. Soc. 137 (2015) (1809) 11801–11811.
[47] J. Reboul, S. Furukawa, N. Horike, M. Tsotsalas, K. Hirai, H. Uehara, M. Kondo, N. Louvain, O. Sakata, S. Kitagawa, Nat. Mater. 11 (2012) 717.
[48] M.L. Foo, R. Matsuda, Y. Hijikata, R. Krishna, H. Sato, S. Horike, A. Hori, J. Duan, Y. Sato, Y. Kubota, J. Am. Chem. Soc. 138 (2016) 3022–3030.
[49] L. Zhu, X.-Q. Liu, H.-L. Jiang, L.-B. Sun, Chem. Rev. (2017).
[50] W. Xuan, C. Zhu, Y. Liu, Y. Cui, Chem. Soc. Rev. 41 (2012) 1677–1695.
[51] T. Toyao, M. Saito, S. Dohshi, K. Mochizuki, M. Iwata, H. Higashimura, Y. Horiuchi, M. Matsuoka, Chem. Commun. 50 (2014) 6779–6781.
[52] R.R. Salunkhe, Y.V. Kaneti, Y. Yamauchi, ACS Nano (2017).
[53] D.-Y. Du, J.-S. Qin, S.-L. Li, Z.-M. Su, Y.-Q. Lan, Chem. Soc. Rev. 43 (2014) 4615–4632.
[54] A. Corma, H. García, F. Llabrés i Xamena, Chem. Rev. 110 (2010) 4606–4655.
[55] W. Xiong, J. Tong, Z. Yang, G. Zeng, Y. Zhou, D. Wang, P. Song, R. Xu, C. Zhang, M. Cheng, J. Colloid Interface Sci. 493 (2017) 17–23.
[56] J.-X. Qin, P. Tan, Y. Jiang, X.-Q. Liu, Q.-X. He, L.-B. Sun, Green Chem. 18 (2016) 3210–3215.
[57] Y. Bai, Y. Dou, L.-H. Xie, W. Rutledge, J.-R. Li, H.-C. Zhou, Chem. Soc. Rev. 45 (2016) 2327–2367.
[58] S.M. Rogge, A. Bavykina, J. Hajek, H. Garcia, A.I. Olivos-Suarez, A. Sepúlveda-Escribano, A. Vimont, G. Clet, P. Bazin, F. Kapteijn, Chem. Soc. Rev. (2017).
[59] H.-C. Zhou, J.R. Long, O.M. Yaghi, in, ACS Publications, 2012.
[60] B. Van de Voorde, B. Bueken, J. Denayer, D. De Vos, Chem. Soc. Rev. 43 (2014) 5766–5788.
[61] M.F. de Lange, K.J. Verouden, T.J. Vlugt, J. Gascon, F. Kapteijn, Chem. Rev. 115 (2015) 12205–12250.
[62] T. Zhang, W. Lin, Chem. Soc. Rev. 43 (2014) 5982–5993.
[63] Z. Wu, X. Yuan, J. Zhang, H. Wang, L. Jiang, G. Zeng, ChemCatChem 9 (2017) 41–64.
[64] M. Wen, K. Mori, Y. Kuwahara, T. An, H. Yamashita, Appl. Catal. B: Environ. 218 (2017) 555–569.
[65] M.-L. Hu, V. Safarifard, E. Doustkhah, S. Rostamnia, A. Morsali, N. Nouruzi, S. Beheshti, K. Akhbari, Microporous Mesoporous Mater. 256 (2018) 111–127.
[66] V.K. Sharma, M. Feng, J. Hazard. Mater. (2017), https://doi.org/10.1016/j.jhazmat.2017.09.043.
[67] P. Railey, Y. Song, T. Liu, Y. Li, Mater. Res. Bull. 96 (2017) 385–394.
[68] Y. Liu, A.J. Howarth, N.A. Vermeulen, S.-Y. Moon, J.T. Hupp, O.K. Farha, Coord. Chem. Rev. 346 (2017) 101–111.
[69] A. Dhakshinamoorthy, A.M. Asiri, H. Garcia, Chem. Commun. 53 (2017) 10851–10869.
[70] M.I. Nandasiri, S.R. Jambovane, B.P. McGrail, H.T. Schaef, S.K. Nune, Coord. Chem. Rev. 311 (2016) 38–52.
[71] J. Zhu, P.-Z. Li, W. Guo, Y. Zhao, R. Zou, Coord. Chem. Rev. 359 (2018) 80–101.
[72] Y.-Z. Chen, R. Zhang, L. Jiao, H.-L. Jiang, Coord. Chem. Rev. 362 (2018) 1–23.
[73] E.M. Dias, C. Petit, J. Mater. Chem. A 3 (2015) 22484–22506.
[74] X. Liu, Y. Zhou, J. Zhang, L. Tang, L. Luo, G. Zeng, ACS Appl. Mater. Inter. 9 (2017) 20255–20275.
[75] S.-N. Zhao, X.-Z. Song, S.-Y. Song, H.-J. Zhang, Coord. Chem. Rev. 337 (2017) 80–96.
[76] P. Falcaro, R. Ricco, A. Yazdi, I. Imaz, S. Furukawa, D. Maspoch, R. Ameloot, J.D. Evans, C.J. Doonan, Coord. Chem. Rev. 307 (2016) 237–254.
[77] D. Wang, M. Wang, Z. Li, ACS Catal. 5 (2015) 6852–6857.
[78] E. Andris, R. Navrátil, J. Jašík, T. Terencio, M. Srnec, M. Costas, J. Roithová, J. Am. Chem. Soc 139 (2017) 2757–2765.
[79] Z. Han, J. Guo, W. Li, Chem. Eng. J. 228 (2013) 36–44.
[80] M. Cheng, W. Ma, C. Chen, J. Yao, J. Zhao, Appl. Catal. B: Environ. 65 (2006) 217–226.
[81] Y. Li, H. Liu, W.-J. Li, F.-Y. Zhao, W.-J. Ruan, RSC Adv. 6 (2016) 6756–6760.
[82] C. Gao, S. Chen, X. Quan, H. Yu, Y. Zhang, J. Catal. 356 (2017) 125–132.
[83] C. Bilgrien, S. Davis, R.S. Drago, J. Am. Chem. Soc. 109 (1987) 3786–3787.
[84] H.E. Toma, K. Araki, A.D. Alexiou, S. Nikolaou, S. Dovidauskas, Coord. Chem. Rev. 219 (2001) 187–234.
[85] H. Lv, H. Zhao, T. Cao, L. Qian, Y. Wang, G. Zhao, J. Mol. Catal. A: Chem. 400 (2015) 81–89.
[86] M. Wang, G. Fang, P. Liu, D. Zhou, C. Ma, D. Zhang, J. Zhan, Appl. Catal. B: Environ. 188 (2016) 113–122.
[87] M. Umar, H.A. Aziz, M.S. Yusoff, Waste Manage. (Oxford) 30 (2010) 2113–2121.
[88] V. Kavitha, K. Palanivelu, Chemosphere 55 (2004) 1235–1243.
[89] N. Klamerth, S. Malato, A. Agüera, A. Fernández-Alba, Water Res. 47 (2013) 833–840.
[90] M.J. Lima, C.G. Silva, A.M. Silva, J.C. Lopes, M.M. Dias, J.L. Faria, Chem. Eng. J. 310 (2017) 342–351.
[91] X. Li, Y. Pi, L. Wu, Q. Xia, J. Wu, Z. Li, J. Xiao, Appl. Catal. B: Environ. 202 (2017) 653–663.
[92] D. Chatterjee, S. Dasgupta, J. Photoch. Photo. C Photoch. Rev. 6 (2005) 186–205.
[93] X. Zhou, J. Lan, G. Liu, K. Deng, Y. Yang, G. Nie, J. Yu, L. Zhi, Angew. Chem. Int. Ed. 124 (2012) 182–186.
[94] K.G.M. Laurier, F. Vermoortele, R. Ameloot, D.E. De Vos, J. Hofkens, M.B.J. Roeffaers, J. Am. Chem. Soc. 135 (2013) 14488–14491.

[95] Y. Gao, S. Li, Y. Li, L. Yao, H. Zhang, Appl. Catal. B: Environ. 202 (2017) 165–174.
[96] K. Liu, Y. Gao, J. Liu, Y. Wen, Y. Zhao, K. Zhang, G. Yu, Environ. Sci. Technol. 50 (2016) 3634–3640.
[97] Y. Gao, G. Yu, K. Liu, S. Deng, B. Wang, J. Huang, Y. Wang, Chem. Eng. J. 330 (2017) 157–165.
[98] C. Zhang, L. Ai, J. Jiang, J. Mater. Chem. A 3 (2015) 3074–3081.
[99] L. Ai, C. Zhang, L. Li, J. Jiang, Appl. Catal. B: Environ. 148 (2014) 191–200.
[100] H. Wang, X. Yuan, Y. Wu, G. Zeng, X. Chen, L. Leng, H. Li, Appl. Catal. B: Environ. 174–175 (2015) 445–454.
[101] Y. Wu, H. Luo, H. Wang, RSC Adv. 4 (2014) 40435–40438.
[102] T.A. Vu, G.H. Le, H.T. Vu, K.T. Nguyen, T.T. Quan, Q.K. Nguyen, H.T. Tran, P.T. Dang, L.D. Vu, G.D. Lee, Mater. Res. Express 4 (2017) 035038.
[103] N.T. Khoa, S.W. Kim, D. Van Thuan, H.N. Tien, S.H. Hur, E.J. Kim, S.H. Hahn, RSC Adv. 5 (2015) 63964–63969.
[104] Y. Shao, L. Zhou, C. Bao, J. Ma, M. Liu, F. Wang, Chem. Eng. J. 283 (2016) 1127–1136.
[105] M. Angamuthu, G. Satishkumar, M. Landau, Microporous Mesoporous Mater. 251 (2017) 58–68.
[106] L. Xu, J. Wang, Environ. Sci. Technol. 46 (2012) 10145–10153.
[107] N.A. Zubir, C. Yacou, J. Motuzas, X. Zhang, J.C.D. Da Costa, Sci. Rep. 4 (2014).
[108] C.-F. Zhang, L.-G. Qiu, F. Ke, Y.-J. Zhu, Y.-P. Yuan, G.-S. Xu, X. Jiang, J. Mater. Chem. A 1 (2013) 14329–14334.
[109] H. Zhao, L. Qian, H. Lv, Y. Wang, G. Zhao, ChemCatChem 7 (2015) 4148–4155.
[110] H. Wang, X. Yuan, Y. Wu, G. Zeng, H. Dong, X. Chen, L. Leng, Z. Wu, L. Peng, Appl. Catal. B: Environ. 186 (2016) 19–29.
[111] S.E. Moradi, S. Dadfarnia, A.M. Haji, S. Shabani, Turkish J. Chem. 41 (2017) 426–439.
[112] L. Zhang, J. Li, Z. Chen, Y. Tang, Y. Yu, Appl. Catal. A: Gen. 299 (2006) 292–297.
[113] K. Choi, W. Lee, J. Hazard. Mater. 211 (2012) 146–153.
[114] I.R. Guimaraes, A. Giroto, L.C. Oliveira, M.C. Guerreiro, D.Q. Lima, J.D. Fabris, Appl. Catal. B: Environ. 91 (2009) 581–586.
[115] M. Chen, P. Xu, G. Zeng, C. Yang, D. Huang, J. Zhang, Biotechnol. Adv. 33 (2015) 745–755.
[116] L. Lyu, L. Zhang, C. Hu, Chem. Eng. J. 274 (2015) 298–306.
[117] L.-J. Han, Y.-J. Kong, T.-J. Yan, L.-T. Fan, Q. Zhang, H.-J. Zhao, H.-G. Zheng, Dalton Trans. 45 (2016) 18566–18571.
[118] S.-Y. Hao, C. Liu, Z.-C. Hao, G.-H. Cui, J. Inorg. Organomet. Polym. Mater. 27 (2017) 105–113.
[119] H.H. Li, Y.J. Ma, Y.Q. Zhao, G.H. Cui, Transition Met. Chem. 40 (2015) 21–29.
[120] R. Yang, Y.G. Liu, K. Van Hecke, G.H. Cui, Transition Met. Chem. 40 (2015) 333–340.
[121] J.M. Hao, Y.H. Li, H.H. Li, G.H. Cui, Transition Met. Chem. 39 (2014) 1–8.
[122] J.C. Geng, L.W. Liu, S.L. Xiao, G.H. Cui, Transition Met. Chem. 38 (2013) 143–148.
[123] R. Yang, K. Van Hecke, B.Y. Yu, G.Y. Li, G.H. Cui, Transition Met. Chem. 39 (2014) 535–541.
[124] X.X. Wang, B. Yu, K. Van Hecke, G.H. Cui, RSC Adv. 4 (2014) 61281–61289.
[125] S.-L. Xiao, Y.-G. Liu, L. Qin, G.-H. Cui, Inorg. Chem. Commun. 36 (2013) 220–223.
[126] C. Racles, M.-F. Zaltariov, M. Iacob, M. Silion, M. Avadanei, A. Bargan, Appl. Catal. B: Environ. 205 (2017) 78–92.
[127] Y. Yao, H. Chen, C. Lian, F. Wei, D. Zhang, G. Wu, B. Chen, S. Wang, J. Hazard. Mater. 314 (2016) 129–139.
[128] L. Wang, Y. Wu, R. Cao, L. Ren, M. Chen, X. Feng, J. Zhou, B. Wang, ACS Appl. Mater. Inter. 8 (2016) 16736–16743.
[129] Q. Sun, M. Liu, K. Li, Y. Han, Y. Zuo, F. Chai, C. Song, G. Zhang, X. Guo, Inorg. Chem. Front. 4 (2017) 144–153.
[130] A. Pariyar, H. Yaghoobnejad Asl, A. Choudhury, Inorg. Chem. 55 (2016) 9250–9257.
[131] H. Wang, X. Yuan, Y. Wu, X. Chen, L. Leng, G. Zeng, RSC Adv. 5 (2015) 32531–32535.
[132] S. Ferlay, T. Mallah, R. Ouahes, P. Veillet, M. Verdaguer, Nature 378 (1995) 701.
[133] L. Zhang, H.B. Wu, X.W. Lou, J. Am. Chem. Soc. 135 (2013) 10664–10672.
[134] L. Qin, G. Zeng, C. Lai, D. Huang, P. Xu, C. Zhang, M. Cheng, X. Liu, S. Liu, B. Li, H. Yi, Coord. Chem. Rev. 359 (2018) 1–31.
[135] X. Li, J. Liu, A.I. Rykov, H. Han, C. Jin, X. Liu, J. Wang, Appl. Catal. B: Environ. 179 (2015) 196–205.
[136] X. Li, A.I. Rykov, J. Wang, Catal. Commun. 77 (2016) 32–36.
[137] X. Li, Z. Wang, B. Zhang, A.I. Rykov, M.A. Ahmed, J. Wang, Appl. Catal. B: Environ. 181 (2016) 788–799.
[138] Y. Ren, L. Lin, J. Ma, J. Yang, J. Feng, Z. Fan, Appl. Catal. B: Environ. 165 (2015) 572–578.
[139] G. Férey, C. Mellot-Draznieks, C. Serre, F. Millange, J. Dutour, S. Surblé, I. Margiolaki, Science 309 (2005) 2040–2042.
[140] T.A. Vu, G.H. Le, C.D. Dao, L.Q. Dang, K.T. Nguyen, P.T. Dang, H.T. Tran, Q.T. Duong, T.V. Nguyen, G.D. Lee, RSC Adv. 4 (2014) 41185–41194.
[141] L. Qin, Z. Li, Z. Xu, X. Guo, G. Zhang, Appl. Catal. B: Environ. 179 (2015) 500–508.
[142] J. Joubert, F. Delbecq, P. Sautet, E.L. Roux, M. Taoufik, C. Thieuleux, F. Blanc, C. Copéret, J. Thivolle-Cazat, J.-M. Basset, J. Am. Chem. Soc. 128 (2006) 9157–9169.
[143] R. Jin, Nanotechnol. Rev. 1 (2012) 31–56.
[144] M. Meilikhov, K. Yusenko, D. Esken, S. Turner, G. Van Tendeloo, R.A. Fischer, Eur. J. Inorg. Chem. 2010 (2010) 3701–3714.
[145] Y. Fu, D. Sun, Y. Chen, R. Huang, Z. Ding, X. Fu, Z. Li, Angew. Chem. Int. Ed. 124 (2012) 3420–3423.
[146] C. Hou, G. Zhao, Y. Ji, Z. Niu, D. Wang, Y. Li, Nano Res. 7 (2014) 1364–1369.
[147] H.-L. Jiang, B. Liu, T. Akita, M. Haruta, H. Sakurai, Q. Xu, J. Am. Chem. Soc. 131 (2009) 11302–11303.
[148] Y.E. Cheon, M.P. Suh, Angew. Chem. Int. Ed. 48 (2009) 2899–2903.
[149] M.S. El-Shall, V. Abdelsayed, S.K. Abd El Rahman, H.M. Hassan, H.M. El-Kaderi, T.E. Reich, J. Mater. Chem. 19 (2009) 7625–7631.
[150] R. Liang, F. Jing, L. Shen, N. Qin, L. Wu, Nano Res. 8 (2015) 3237–3249.
[151] R. Liang, S. Luo, F. Jing, L. Shen, N. Qin, L. Wu, Appl. Catal. B: Environ. 176 (2015) 240–248.
[152] R. Marschall, Adv. Funct. Mater. 24 (2014) 2421–2440.
[153] S. Yang, Y. Gong, J. Zhang, L. Zhan, L. Ma, Z. Fang, R. Vajtai, X. Wang, P.M. Ajayan, Adv. Mater. 25 (2013) 2452–2456.
[154] W. Cho, S. Park, M. Oh, Chem. Commun. 47 (2011) 4138–4140.
[155] X. Yan, X. Li, Z. Yan, S. Komarneni, Appl. Surf. Sci. 308 (2014) 306–310.
[156] C. Bao, H. Zhang, L. Zhou, Y. Shao, J. Ma, Q. Wu, RSC Adv. 5 (2015) 72423–72432.
[157] X. Li, Z. Ao, J. Liu, H. Sun, A.I. Rykov, J. Wang, ACS Nano 10 (2016) 11532–11540.
[158] M. Zeng, Y. Liu, F. Zhao, K. Nie, N. Han, X. Wang, W. Huang, X. Song, J. Zhong, Y. Li, Adv. Funct. Mater. 26 (2016) 4397–4404.
[159] Y. Yang, Z. Lun, G. Xia, F. Zheng, M. He, Q. Chen, Energy Environ. Sci. 8 (2015) 3563–3571.
[160] B.K. Barman, K.K. Nanda, Green Chem. 18 (2016) 427–432.
[161] H. Wang, X. Yuan, Y. Wu, G. Zeng, X. Chen, L. Leng, Z. Wu, L. Jiang, H. Li, J. Hazard. Mater. 286 (2015) 187–194.
[162] C. Cai, H. Zhang, X. Zhong, L. Hou, J. Hazard. Mater. 283 (2015) 70–79.
[163] M. Cheng, G. Zeng, D. Huang, C. Lai, Y. Liu, C. Zhang, J. Wan, L. Hu, C. Zhou, W. Xiong, Water Res. 138 (2018) 7–18.
[164] D. He, J. Ma, R.N. Collins, T.D. Waite, Environ. Sci. Technol. 50 (2016) 3820–3828.
[165] X. Tan, Y. Liu, G. Zeng, X. Wang, X. Hu, Y. Gu, Z. Yang, Chemosphere 125 (2015) 70–85.
[166] C. Zhang, C. Lai, G. Zeng, D. Huang, C. Yang, Y. Wang, Y. Zhou, M. Cheng, Water Res. 95 (2016) 103–112.
[167] C. Zhou, C. Lai, D. Huang, G. Zeng, C. Zhang, M. Cheng, L. Hu, J. Wan, W. Xiong, M. Wen, X. Wen, L. Qin, Appl. Catal. B: Environ. 220 (2018) 202–210.
[168] Y. Liu, G. Zeng, H. Zhong, Z. Wang, Z. Liu, M. Cheng, G. Liu, X. Yang, S. Liu, J. Hazard. Mater. 322 (2017) 394–401.
[169] C. Lai, M.-M. Wang, G.-M. Zeng, Y.-G. Liu, D.-L. Huang, C. Zhang, R.-Z. Wang, P. Xu, M. Cheng, C. Huang, H.-P. Wu, L. Qin, Appl. Surf. Sci. 390 (2016) 368–376.
[170] K. Li, Y. Zhao, M.J. Janik, C. Song, X. Guo, Appl. Surf. Sci. 396 (2017) 1383–1392.
[171] J. De Laat, H. Gallard, Environ. Sci. Technol. 33 (1999) 2726–2732.
[172] M. Cheng, G. Zeng, D. Huang, L. Liu, M. Zhao, C. Lai, C. Huang, Z. Wei, N. Li, P. Xu, Biochem. Eng. J. 84 (2014) 9–15.
[173] X. Hu, B. Liu, Y. Deng, H. Chen, S. Luo, C. Sun, P. Yang, S. Yang, Appl. Catal. B: Environ. 107 (2011) 274–283.
[174] H. Zhao, Y. Chen, Q. Peng, Q. Wang, G. Zhao, Appl. Catal. B: Environ. 203 (2017) 127–137.